ChemComm

Cite this: *Chem. Commun.*, 2011, **47**, 7194–7196

www.rsc.org/chemcomm

COMMUNICATION



# Irreversible solvent-driven conversion in cyanometalate $\{Fe_2Ni\}_n$ ($n$ = 2, 3) single-molecule magnets†

**Yuan-Zhu Zhang,[a] Uma P. Mallik,[a] Rodolphe Clérac,*[bc] Nigam P. Rath[a] and Stephen M. Holmes*[ad]**

***Received 3rd February 2011, Accepted 28th April 2011***
**DOI: 10.1039/c1cc10679a**

**Two cyano-bridged single-molecule magnets of $\{Fe^{III}_4Ni^{II}_2\}$ and $\{Fe^{III}_6Ni^{II}_3\}$ stoichiometry are described *via* their magnetic properties described in the frame of geometrical core distortions and orientations of their local anisotropy axes.**

Cyano-bridged assemblies remain an active area of research owing to their ability to exhibit tunable physical properties.[1–3] Using a building-block approach, molecular precursors are allowed to self-assemble towards a common structural archetype *via* the formation of M(μ-CN)M′ pairs. Using a variety of multidentate capping ligands, the directionality and numbers of coordination sites available for M(μ-CN)M′ unit formation can be controlled at the single-ion level. This strategy allows for the preparation of structurally related polynuclear materials with tailored magnetic and optical properties like single-molecule magnets (SMMs),[1] single-chain magnets (SCMs),[2] and photo-responsive complexes.[3]

Over the last 5 years we have striven to systematically prepare cyanide-bridged SMMs derived from poly(pyrazolyl)borate tricyanometalates by tuning ancillary ligand steric demand. This approach allows for the isolation of several tri-, tetra-, and octanuclear complexes exhibiting a range of remarkable properties.[1d,e,i–k,3b,d] For example, rod-shaped $\{Fe^{III}_4Ni^{II}_4\}$ complexes exhibit much higher SMM energy barriers ($\Delta/k_B$ = 33 K) in comparison to more symmetrical molecular boxes, due to a better alignment of their anisotropy tensors.[1i,j] Surprisingly, while several hexanuclear $\{Fe^{III}_2M^{II}\}_2$ complexes containing $[(Tp)Fe(CN)_3]^-$ anions are known (Tp = trispyrazoylborate), none are reported to exhibit SMM properties;[4] higher nuclearity $\{Fe^{III}_2Ni^{II}\}_n$ ($n \geq 3$) analogues are also unknown. As part of our efforts to engineer polynuclear SMMs, we now report a general methodology for the preparation of hexa- and nona-nuclear $\{Fe^{III}_2Ni^{II}\}_n$ complexes that exhibit SMM behavior.

Treatment of $[NEt_4][(Tp^{*Me})Fe(CN)_3]\cdot H_2O$[1t] with $NiCl_2$ in a 2 : 1 molar ratio in DMF, followed by addition of $Et_2O$ readily affords $\{[(Tp^{*Me})Fe^{III}(CN)_3]_4[Ni^{II}(DMF)_3]_2\}\cdot 4DMF\cdot H_2O$ (**1**) as red blocks ($Tp^{*Me}$ = tris(3,4,5-trimethylpyrazole)borate). The infrared spectrum of **1** exhibits several strong $\bar{\nu}_{CN}$ absorptions (2173, 2148, 2115 $cm^{-1}$) that are shifted to higher energies relative to those seen for $[NEt_4][(Tp^{*Me})Fe(CN)_3]\cdot H_2O$ (2119, 2115 $cm^{-1}$), indicating that both bridging and terminal cyanides are present. Surprisingly, using MeOH as a reaction solvent or alternatively, dissolving crystalline samples of **1** into MeOH, a second complex $\{[(Tp^{*Me})Fe^{III}(CN)_3]_6\ [Ni^{II}(MeOH)_3]_2[Ni^{II}(MeOH)_2]\}\cdot 3H_2O\cdot 8MeOH$ (**2**) is obtained. Attempts to obtain **1** from either DMF or MeOH solutions of **2** were unsuccessful suggesting that the Fe(μ-CN)Ni units are fragile and that MeOH hydrogen bonding interactions play a role in the fragmentation of **1** and concomitant reassembly of the constituent building blocks to form **2**.‡ The $\bar{\nu}_{CN}$ stretches (2165, 2121 $cm^{-1}$) seen for **2** differ from those found for **1**, indicating that the electronic environments of the cyanides have been altered.

Compound **1** crystallizes in the triclinic $P\bar{1}$ space group as a centrosymmetric hexanuclear complex (Fig. 1, S1–S2; Tables S1–S2),† that contains a central two-connected $\{[(Tp^{*Me})Fe^{III}(CN)_3]_2[Ni^{II}(DMF)_3]_2\}$ square connected *via* $Fe^{III}$(μ-CN)$Ni^{II}$ linkages to $[(Tp^{*Me})Fe(CN)_3]^-$ fragments. The structure of **1** resembles the $\{Fe^{III}_2Ni^{II}\}$ repeat unit found in a variety of {4,2}-ribbons of $[\{Fe^{III}(L)(CN)_4\}_2Ni^{II}(H_2O)_2]\cdot 4H_2O$ (L = 2,2′-bipyridine, 1,10-phenanthroline) stoichiometry.[2e] In **1**, the $Fe^{III}$ and $Ni^{II}$ centers adopt distorted octahedral geometries and exhibit Fe–C, Fe–N and Ni–N/O bond lengths that range between 1.901(4) to 1.927(4) Å, 1.983 to 2.000(3), and 2.001(3) to 2.100(3) Å, respectively. Within the $Fe^{III}$(μ-CN)$Ni^{II}$ units, the cyanides are nearly linear with respect to the Fe centers and Fe–C–N angles ranging between 172.9(3)° and 178.2(4)° are found while the Ni–N–C angles range between 170.2(3)° and 177.1(3)°. The $\{Fe_4Ni_2\}$ cores in **1** are well-separated and closest inter-complex Fe···Ni contacts of 8.71(1) Å are found.

Compound **2** crystallizes in the monoclinic $C2/c$ space group as a nonanuclear complex whose core resembles the $\{Fe^{III}_2Ni^{II}\}_3$ fragments seen in a variety of {4,2} one-dimensional chains[2a,b,e] (Tables S1–S2, Fig. 2, S3 and S4).† Within the central core of **2** the $[(Tp^{*Me})Fe(CN)_3]^-$ fragments [Fe1 and Fe2] are linked to adjacent $Ni^{II}$ ions *via* two bridging cyanides and the two

[a] *Department of Chemistry and Biochemistry, University of Missouri-St. Louis, St. Louis, Missouri 63121, USA. E-mail: holmesst@umsl.edu; Fax: (+1) 314 516 5342; Tel: (+1) 314 516 4382*
[b] *CNRS, UPR 8641, Centre de Recherche Paul Pascal (CRPP), Equipe "Matériaux Moléculaires Magnétiques", 115 avenue du Dr Albert Schweitzer, Pessac, F-33600, France. E-mail: clerac@crpp-bordeaux.cnrs.fr; Fax: (+33) 5 56 84 56 00; Tel: (+33) 5 56 84 56 50*
[c] *Université de Bordeaux, UPR 8641, Pessac, F-33600, France*
[d] *Center for Nanoscience, University of Missouri-St. Louis, St. Louis, Missouri 63121, USA*

† Electronic supplementary information (ESI) available: Additional crystallographic and magnetic data. CCDC 810415 (**1**) and 810416 (**2**). For ESI and crystallographic data in CIF or other electronic format see DOI: 10.1039/c1cc10679a

 

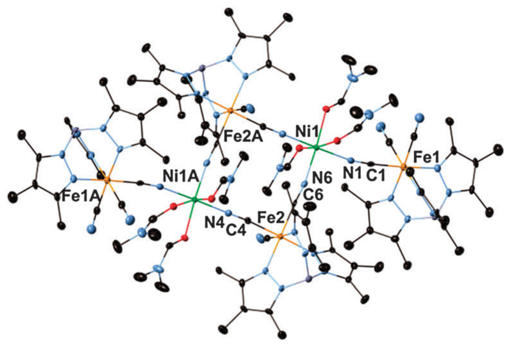


**Fig. 1** X-ray structure of **1**. Thermal ellipsoids are at the 50% level and all lattice solvent and hydrogen atoms are eliminated for clarity.

$\{Fe^{III}{}_2Ni^{II}{}_2\}$ squares share a common and central $Ni^{II}$ center (Ni1); the remaining terminal cyanides adopt *anti* orientations with respect to the mean $\{Fe^{III}{}_2Ni^{II}{}_2\}$ plane. Additional symmetry-related $Fe^{III}$(μ-CN)$Ni^{II}$ units (Fe3-C8-N8-Ni2) link the remaining $[(Tp^{*Me})Fe(CN)_3]^-$ anions and complete the structure of the neutral complex. The metal ions in **2** adopt more distorted coordination geometries in comparison to those seen in **1** and average Fe–C, Fe–N, Ni–O and Ni–N distances of *ca.* 1.919(6), 1.988(4), 2.115(5) and 2.023(5) Å are found. The Fe–C–N and Ni–N–C angles are also in comparison more distorted than those in **1**, ranging between 171.6(5) and 177.4(7)° and 157.5(4) and 172.8(4)°. The $\{Fe_6Ni_3\}$ cores in **2** are well-isolated from adjacent ones as the closest intercomplex Fe···Fe contacts of 9.26(1) Å are found.

Further inspection of both $\{Fe^{III}{}_2Ni^{II}\}_n$ cores indicates that **2** adopts a rather twisted conformation in comparison to **1**. The mean plane deviations of the $\{Fe_2Ni_2\}$ squares in **1** and **2** are small [*ca.* 0.02 Å avg.] but in **2**, a pronounced dihedral twisting [*ca.* 33.1(1)°] of the $\{Fe_2Ni_2\}$ squares about Ni1 is found. Concomitantly, the pseudo-$C_3$ axes (along the B···Fe vectors) adopt different orientations [up to 58.6(1)°] within the square $\{Fe_2Ni_2\}$ units in **2**, while those in **1** are parallel (Fig. S1–S4).†

Considering that the pseudo-$C_3$ rotation axes on $Fe^{III}$ are structural markers for the anisotropy tensors we hypothesized that a parallel arrangement of these would likely afford complexes with high SMM energy barriers within a given system. To investigate this assumption we began a series of magnetic measurements to determine whether **1** and **2** would follow this qualitative trend.[1d–g,i–k,5] The room temperature $\chi T$ values for **1** and **2** [4.8 and 8.8 cm$^3$ K mol$^{-1}$, respectively] confirm that $Fe^{III}{}_{LS}$ ($S=\frac{1}{2}$) and $Ni^{II}$ ($S$ = 1) ions are present in a 4 : 2 and 6 : 3 ratio assuming that $g_{Fe}$ ~2.6–2.7 and $g_{Ni}$ ~2.1–2.2. As the temperature is lowered (Fig. 3, S5),† the $\chi T$ products increase towards maximum values of 14.4 and 31.5 cm$^3$ K mol$^{-1}$ at 3.7 and 3.9 K (for **1** and **2**), signaling that ferromagnetic exchange is operative between the $Fe^{III}$ and $Ni^{II}$ centers, as is typical in a variety of cyanide-based $Fe^{III}/Ni^{II}$ materials;[1d,e,g,h–l,2e] at lower temperatures minimum $\chi T$ values of 14.0 and 29.5 cm$^3$ K mol$^{-1}$ at 1.8 K are found for **1** and **2**.

On the basis of the structures of **1** and **2**, the magnetic data were simulated numerically[6] using the following isotropic Heisenberg spin Hamiltonians: $H = -2J_1[S_{Ni1}\cdot(S_{Fe1} + S_{Fe2} + S_{Fe2A}) + S_{Ni1A}\cdot(S_{Fe1A} + S_{Fe2} + S_{Fe2A}]$ for **1** and $H = -2J_2[S_{Ni1}\cdot(S_{Fe1} + S_{Fe2} + S_{Fe1A} + S_{Fe2A}) + S_{Ni2}\cdot(S_{Fe1} + S_{Fe2} + S_{Fe3}) + S_{Ni2A}\cdot(S_{Fe1A} + S_{Fe2A} + S_{Fe3A})]$ for **2**, where $J_1$ and $J_2$ represent the average exchange interactions between $Fe^{III}$ ($S = \frac{1}{2}$) and $Ni^{II}$ ($S$ = 1) spin centers. The best simulations of the data (Fig. 3) were obtained between 300 and 12 K, and average values of $J_1/k_B$ = +9.0(5) K and $g_{avg(1)}$ = 2.3(1) and $J_2$ = +9.0(5) K and $g_{avg(2)}$ = 2.5(1) were deduced for **1** and **2**, respectively. These values are comparable to those reported for related $\{Fe^{III}{}_nNi^{II}{}_m\}$ complexes.[1d,e,g–l] Attempts to incorporate more terms, different $J$ or g factors, or single-ion anisotropy did not improve the simulation of the data below *ca.* 12 K, suggesting that all or a combination of the above factors are likely manifested below *ca.* 12 K.

The field dependencies of the magnetization have also been measured (Inset of Fig. 3, Fig. S6–S7) to investigate the overall spin ground states of **1** and **2**.† Even under 7 T at 1.8 K, the magnetization values [6.9 and 14.0 $\mu_B$] for **1** and **2** are not fully saturated suggesting that significant magnetic anisotropy is present. Nevertheless, high field magnetizations support the assumption that $S_T$ = 4 and 6 spin ground states (with $g_{av}$ > 2) for **1** and **2** are present and is consistent with the $\chi T$ *vs.* $T$ data. Attempts to fit the $M$ *vs.* $H$ data using $S_T$ = 4 and 6 macro-spin models (with $H = DS_{T,z}{}^2$) leads to unrealistic magnetic parameters ($D/k_B < -6$ K, inset Fig. 3 for **1**) suggesting that $S_T$ is not exclusively populated even at 1.8 K for each complex.

To further investigate the apparent anisotropy seen for **1** and **2**, ac susceptibility measurements were obtained. Indeed both **1** and **2** exhibit strong frequency-dependent behavior in their ac susceptibility data (Fig. 4, S8–S11).† As shown in Fig. 4 (left; Fig. S10–S11),† **1** and **2** exhibit SMM behavior consistent with a

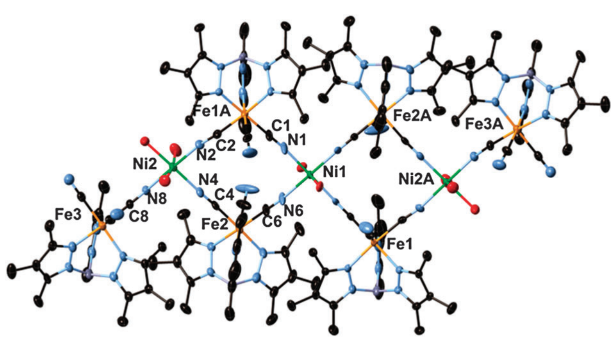


**Fig. 2** X-ray structure of **2**. Thermal ellipsoids are at the 50% level and all lattice solvent, hydrogen atoms, and MeOH methyl groups are eliminated for clarity.

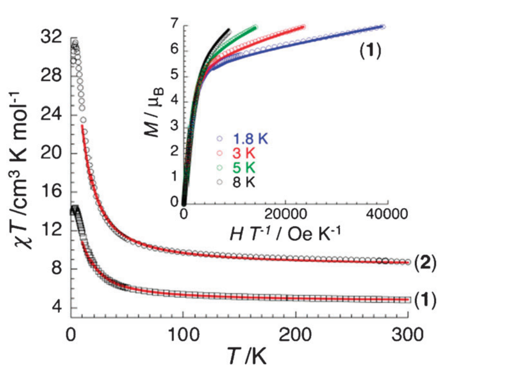


**Fig. 3** $\chi T$ *vs.* $T$ data for **1** and **2** at 1000 Oe ($\chi$ being the magnetic susceptibility equal to $M/H$). Solid lines represent the best simulations down to 12 K (see text). Inset: $M$ *vs.* $H\ T^{-1}$ for **1**.

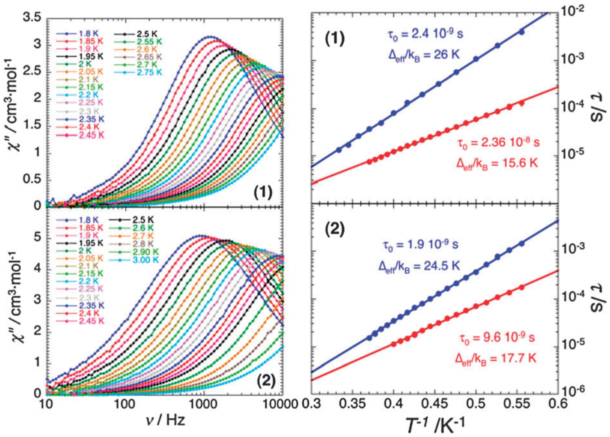


**Fig. 4** Left: $\chi''$ *vs.* $\nu$ data in zero *dc* field and an *ac* field of 1 Oe at various temperatures for **1** (top, left) and **2** (bottom, left), respectively. Right: Semi-logarithmic $\tau$ *vs.* $1/T$ plot at zero *dc* field (•), at 1500 Oe (•) for **1** (top, right) and at 600 Oe (•) for **2** (bottom, right), respectively. The solid lines are the best fits with an Arrhenius law.

single mode of relaxation. The deduced relaxation times (Fig. 4, right) follow Arrhenius behavior [$\tau = \tau_0 \exp(\Delta_{eff}/k_BT)$] and effective energy barriers of 15.6 and 17.7 K and pre-exponential terms, $\tau_o$, of $2.4 \times 10^{-8}$ and $9.6 \times 10^{-9}$ s are found for **1** and **2**, respectively. These Arrhenius parameters are comparable to several reported SMMs,[1] but as is the case with many, quantum tunneling of the magnetization (QTM) might be significantly reduced $\Delta_{eff}$.

In order to probe QTM, effective barrier heights, and the relaxation dynamics seen for **1** and **2**, additional ac measurements were initiated. If QTM is present, small dc-fields are expected to lift the degeneracy of the $\pm m_S$ states and decrease the probability of quantum tunneling, thus increasing relaxation times. Indeed application of dc fields cause dramatic reductions in the characteristic frequency from 1213 to 30 Hz ($H_{dc}$ = 1500 Oe) and 1470 to 215 Hz ($H_{dc}$ = 600 Oe), for **1** and **2**, respectively (Fig. S13–S15).† Higher SMM barriers [26 and 24.5 K] and smaller $\tau_o$ [$2.4 \times 10^{-9}$ and $1.9 \times 10^{-9}$ s] are also found allowing for a crude estimation of the anisotropy terms: $D/k_B = -1.6$ and $-0.7$ K for **1** and **2**, respectively (Fig. 4, S16–S19).† The thermally activated energy barriers are comparable for **1** and **2** despite differences in their nuclearity and overall spin ground states ($S_T$ = 4 and 6). These results support that the hypothesis that better alignment of anisotropic ions in **1** (*vide supra*) in comparison to **2**, efficiently increases the magnetic anisotropy ($D$) while simultaneously compensating for a lower spin ground state, affording complexes with similar energy barriers.

In summary, we have shown that solvent choice is an important consideration for constructing polynuclear complexes and controlling their aggregation state. The structural and magnetic data also suggests that controlling the relative orientations of the anisotropy tensors, rather than only the total spin, is an important consideration for designing cyanometalate-based SMMs with appreciable energy barriers.

The authors gratefully acknowledge the National Science Foundation (CHE 0914935, CAREER; CHE 0939987, X-ray upgrade), University of Missouri-St. Louis, the University of Bordeaux, the ANR (NT09_469563, AC-MAGnets project), the Région Aquitaine (GIS Advanced Materials in Aquitaine; COMET) and the CNRS (PICS N° 14659) for financial support.

## Notes and references

‡ Synthesis of **1**: Treatment of $[NEt_4][(Tp^{*Me})Fe(CN)_3]\cdot H_2O$ (186.0 mg, 0.299 mmol) with $NiCl_2\cdot 6H_2O$ (47.2 mg, 0.198 mmol) in a 2 : 1 ratio in DMF (10 mL) afforded a dark red solution that was stirred for 20 min. The mixture was filtered, layered with $Et_2O$ (50 ml), and allowed to stand 7 days. The red rods were isolated *via* filtration, washed with DMF (3 ml), and dried under vacuum for 2 min at room temperature. Yield: 198.0 mg (48.1%). Anal. calcd for $C_{114}H_{180}N_{46}O_{10}B_4Ni_2Fe_4$ (**1**-$H_2O$): C 49.99; H 6.64; N 23.51. Found: C, 49.90; H, 6.81; N, 23.28. IR (Nujol, $cm^{-1}$): 2528 ($\bar{\nu}_{BH}$, m), 2173 ($\bar{\nu}_{CN}$, s), 2148, 2115 ($\bar{\nu}_{CN}$, m). Synthesis of **2**: Treatment of $[NEt_4][(Tp^{*Me})Fe^{III}(CN)_3]\cdot H_2O$ (188.0 mg, 0.303 mmol) in MeOH (20 ml) with $NiCl_2\cdot 6H_2O$ (43.5 mg, 0.183 mmol) in MeOH (20 mL) afforded a dark red solution, which was filtered and allowed to stand 7 days. The red blocks were isolated *via* filtration, washed with methanol (5 mL), and dried under vacuum for 2 min at room temperature. Yield: 115.1 mg (64.1%). Anal. Calcd $C_{136}H_{214}B_6Fe_6N_{54}Ni_3O_{12}$ (**2**-4MeOH): C 48.67; H 6.88; N 22.20. Found: C, 46.90; H, 6.50; N, 22.02. IR (Nujol, $cm^{-1}$): 2533 ($\nu_{BH}$, m), 2165 ($\nu_{CN}$, s), 2121 ($\nu_{CN}$, m). Dissolution of **1** into MeOH also affords crystals of **2** within days.

1 (*a*) J. J. Sokol, A. G. Hee and J. R. Long, *J. Am. Chem. Soc.*, 2002, **124**, 7656–7657; (*b*) L. M. C. Beltran and J. R. Long, *Acc. Chem. Res.*, 2005, **38**, 325–334; (*c*) M. Shatruk, C. Avendano and K. R. Dunbar, *Prog. Inorg. Chem.*, 2009, **56**, 273–279; (*d*) D.-F. Li, S. Parkin, G.-B. Wang, G. T. Yee, A. V. Prosvirin and S. M. Holmes, *Inorg. Chem.*, 2005, **44**, 4903–4905; (*e*) D.-F. Li, R. Clérac, G.-B. Wang, G. T. Yee and S. M. Holmes, *Eur. J. Inorg. Chem.*, 2007, 1341–1346; (*f*) M. Shatruk, A. Dragulescu-Andrasi, K. E. Chambers, S. A. Stoian, E. L. Bominaar, C. Achim and K. R. Dunbar, *J. Am. Chem. Soc.*, 2007, **129**, 6104–6116; (*g*) C.-F. Wang, W. Liu, Y. Song, X.-H. Zhou, J.-L. Zuo and X.-Z. You, *Eur. J. Inorg. Chem.*, 2008, 717–727; (*h*) D.-Y. Wu, Y. J. Zhang, W. Huang and O. Sato, *Dalton Trans.*, 2010, **39**, 5500–5503; (*i*) D.-F. Li, S. Parkin, G.-B. Wang, G. T. Yee, R. Clérac, W. Wernsdorfer and S. M. Holmes, *J. Am. Chem. Soc.*, 2006, **128**, 4214–4215; (*j*) Y.-Z. Zhang, U. P. Mallik, N. Rath, G. T. Yee, R. Clérac and S. M. Holmes, *Chem. Commun.*, 2010, **46**, 4953–4955; (*k*) D.-F. Li, R. Clérac, S. Parkin, G. Wang, G. T. Yee and S. M. Holmes, *Inorg. Chem.*, 2006, **45**, 5251–5253.
2 (*a*) L. M. Toma, R. Lescouëzec, J. Pasán, C. Ruiz-Pérez, J. Vaissermann, J. Cano, R. Carrasco, W. Wernsdorfer, F. Lloret and M. Julve, *J. Am. Chem. Soc.*, 2006, **128**, 4842–4853; (*b*) Y.-J. Zhang, T. Liu, S. Kanegawa and O. Sato, *J. Am. Chem. Soc.*, 2010, **132**, 8250–8251; (*c*) S. Wang, J.-L. Zuo, S. Gao, Y. Song, H.-C. Zhou, Y.-Z. Zhang and X.-Z. You, *J. Am. Chem. Soc.*, 2004, **126**, 8900–8901; (*d*) H.-R. Wen, C.-F. Wang, Y. Song, S. Gao, J.-L. Zuo and X.-Z. You, *Inorg. Chem.*, 2006, **45**, 8942–8949; (*e*) L. M. Toma, R. Lescouëzec, S. Uriel, R. Llusar, C. Ruiz-Pérez, J. Vaissermann, F. Lloreta and M. Julve, *Dalton Trans.*, 2007, 3690–3698; (*f*) T. D. Harris, M. V. Bennett, R. Clérac and J. R. Long, *J. Am. Chem. Soc.*, 2010, **132**, 3980–3988.
3 (*a*) O. Sato, J. Tao and Y.-Z. Zhang, *Angew. Chem., Int. Ed.*, 2007, **46**, 2152–2187; (*b*) D. Li, R. Clérac, O. Roubeau, E. Harté, C. Mathonière, R. Le Bris and S. M. Holmes, *J. Am. Chem. Soc.*, 2008, **130**, 252–258; (*c*) A. Bleuzen, V. Marvaud, C. Mathonière, B. Sieklucka and M. Verdaguer, *Inorg. Chem.*, 2009, **48**, 3453–3466; (*d*) Y.-Z. Zhang, D. Li, R. Clérac, M. Kalisz, C. Mathonière and S. M. Holmes, *Angew. Chem., Int. Ed.*, 2010, **49**, 3752–3756.
4 (*a*) J. Kim, S. Han, K. I. Pokhodnya, J. M. Migliori and J. S. Miller, *Inorg. Chem.*, 2005, **44**, 6983–6988; (*b*) Y.-J. Zhang, T. Liu, S. Kanegawa and O. Sato, *J. Am. Chem. Soc.*, 2009, **131**, 7942–7943.
5 (*a*) K. Park and S. M. Holmes, *J. Phys. Chem. B.: Condens. Mater. Phys.*, 2006, **74**, 224440; (*b*) C.-F. Wang, J.-L. Zuo, B. M. Bartlett, Y. Song, J. R. Long and X.-Z. You, *J. Am. Chem. Soc.*, 2006, **128**, 7162–7163.
6 (*a*) J. J. Borrás-Almenar, J. M. Clemente-Juan, E. Coronado and B. S. Tsukerblat, *Inorg. Chem.*, 1999, **38**, 6081–6088; (*b*) J. J. Borrás-Almenar, J. M. Clemente-Juan, E. Coronado and B. S. Tsukerblat, *J. Comput. Chem.*, 2001, **22**, 985–991.



 